

Development and validation of a canine radius replica for mechanical testing of orthopedic implants

Jeffrey P. Little, DVM; Timothy J. Horn, MS; Denis J. Marcellin-Little, DEDV; Ola L. A. Harrysson, PhD; Harvey A. West II, PhD

Objective—To design and fabricate fiberglass-reinforced composite (FRC) replicas of a canine radius and compare their mechanical properties with those of radii from dog cadavers.

Sample—Replicas based on 3 FRC formulations with 33%, 50%, or 60% short-length discontinuous fiberglass by weight (7 replicas/group) and 5 radii from large (> 30-kg) dog cadavers.

Procedures—Bones and FRC replicas underwent nondestructive mechanical testing including 4-point bending, axial loading, and torsion and destructive testing to failure during 4-point bending. Axial, internal and external torsional, and bending stiffnesses were calculated. Axial pullout loads for bone screws placed in the replicas and cadaveric radii were also assessed.

Results—Axial, internal and external torsional, and 4-point bending stiffnesses of FRC replicas increased significantly with increasing fiberglass content. The 4-point bending stiffness of 33% and 50% FRC replicas and axial and internal torsional stiffnesses of 33% FRC replicas were equivalent to the cadaveric bone stiffnesses. Ultimate 4-point bending loads did not differ significantly between FRC replicas and bones. Ultimate screw pullout loads did not differ significantly between 33% or 50% FRC replicas and bones. Mechanical property variability (coefficient of variation) of cadaveric radii was approximately 2 to 19 times that of FRC replicas, depending on loading protocols.

Conclusions and Clinical Relevance—Within the range of properties tested, FRC replicas had mechanical properties equivalent to and mechanical property variability less than those of radii from dog cadavers. Results indicated that FRC replicas may be a useful alternative to cadaveric bones for biomechanical testing of canine bone constructs. (*Am J Vet Res* 2012;73:27–33)

Biomechanical testing of novel orthopedic implants is often performed in vitro by use of materials testing machines.¹ Cadaveric bones are commonly used for the biomechanical testing of implants. The size, shape, and properties of cadaveric bones typically allow a close approximation of in vivo scenarios. Also, they are often available as matched pairs, facilitating direct comparisons between surgeries performed on the left and right limbs. The use of cadaveric bones for the mechanical evaluation of orthopedic implants has several disadvan-

ABBREVIATIONS

CT	Computed tomography
FRC	Fiberglass-reinforced composite

tages, including high intersample variability, biological degradation, and a lack of availability. These disadvantages may lead to poor experimental consistency.² In 1 study,³ the variability in mechanical properties among long bones from Greyhound cadavers ranged from 7.2% to 62%.

The high variability in cadaveric bone properties necessitates the use of large sample sizes to detect small differences between implants or surgical methods. Substitute materials that simulate the mechanical properties of cortical and cancellous bone have been used to reduce this variability and the required sample size. They include wood, polymers (eg, polyacetal and polyvinyl chloride), and phenolic resin-laminated sheets.^{4–7} Although various materials appear suitable for simulating specific bone properties, their lack of realistic bone geometry complicates the evaluation of implants. Composite bone replicas that mimic the shape and properties of real bones such

Received June 24, 2010.

Accepted November 18, 2010.

From the Department of Clinical Sciences, College of Veterinary Medicine (Little, Marcellin-Little) and the Edward P. Fitts Department of Industrial and Systems Engineering, College of Engineering (Horn, Harrysson, West), North Carolina State University, Raleigh, NC 27606. Dr. Little's present address is Department of Surgical Sciences, School of Veterinary Medicine, University of Wisconsin, Madison, WI 53706.

Supported by the Biomechanical Laboratory, Edward P. Fitts Department of Industrial and Systems Engineering, North Carolina State University.

Address correspondence to Dr. Marcellin-Little (denis_marcellin@ncsu.edu).

as human femora have been developed and are now commercially available.⁸ Some of these composite bones are made of epoxy resin reinforced with a braided tube of glass fibers. Their stiffness is significantly lower than that of cadaveric bone.⁹ Other composite bones are made by use of glass fiber fabric–reinforced epoxy, which have axial and bending stiffnesses similar to those of cadaveric bone but torsional stiffness greater than that of cadaveric bone.^{10,11} The mechanical properties of these human composite femora have an approximately 20-fold smaller variance than that of cadaveric femora.¹⁰ More recently, composite bones have been constructed by use of short-length, discontinuous, fiberglass-reinforced epoxy resin that is molded around a polyurethane foam core.^{8,12} These composite bones may be sawed and broached. They have mechanical properties that closely resemble those of natural human bones, have comparatively low inter-sample variability, and are easy to manufacture.¹³ Among bones from dog cadavers, large variability in mechanical properties has been identified.³ Also, a variability in bone mineral content (ranging from 40% to 60% of the mean value) was present in long bones obtained from cadavers of 36 dogs that were 3 to 10 years of age.¹⁴ Information on the design, fabrication, and validation of composite canine bones is lacking.

The purpose of the study reported here was to design and fabricate FRC replicas of canine radii and to compare their mechanical properties with those of bones from dog cadavers. We hypothesized that increasing the amount of short-length glass fibers in the epoxy resin would increase the axial, bending, and torsional stiffnesses of the composite bone replicas. We also hypothesized that the composite bone replicas would have mechanical properties comparable with those of cadaveric canine radii but with lower mechanical property variability among specimens.

Materials and Methods

Design—Sample sizes were determined with an a priori power analysis by use of statistical software.^{15a} The power analysis was based on sample variability from composite bone models used in a previous study¹⁶ by our research group. Sample sizes were chosen to detect a 25% change in mechanical properties of the composite bones at a power of 0.8.

Sample collection—Forelimbs of 13 adult dogs weighing > 30 kg were collected after euthanasia. The dogs were euthanized at a local animal shelter as part of population control programs. Age, breed, sex, and method of euthanasia were recorded. For each cadaver, both thoracic limbs were disarticulated at the glenohumeral joints, wrapped in saline (0.9% NaCl) solution–moistened gauze, sealed in a plastic bag, and frozen at -20°C . The limbs were thawed at room temperature (approx 23°C), and the radii were removed. Bones were to be excluded from the study when osteoarthritis of the elbow or carpal joints, angular deformities, or signs of prior fracture were visible.

Composite bone design and fabrication—Five pairs of cadaver limbs were thawed at room temperature. Computed tomography of these limbs was performed by use of a helical multislice CT^b (0° gantry tilt; matrix size, 512×512 ; penetrability, 120 kVp; and intensity [determined on the basis of x-ray tube current], 110 mA). The CT images were retroreconstructed into 1-mm slices with a pixel size of 0.727×0.727 mm by use of a sharp convolution kernel (B60s) and a sinus window.¹⁷ This convolution kernel is recommended for CT imaging of extremities in children.¹⁸ The radial geometry of each sample was isolated and reconstructed into 3-D models with modeling software.^c One radius from a 35-kg Rottweiler was chosen at random, and plastic models of the cancellous and cortical bone were created via stereolithography.^d The models had extensions at their proximal and distal aspects that ensured proper positioning and allowed injections during fabrication (Figure 1). The plastic models were used to create silicone rubber molds for the fabrication of the cancellous core and the cortical shell of the composite bones.^e Two molds were created to increase the production rate of FRC replicas. Two-part polyurethane foam with a density of 0.25 g/cm^3 (16 lb/ft^3) mixed in a 1:1 ratio was injected into the cancellous bone mold at room temperature and 42% relative humidity to create the cancellous bone analog.^f The cancellous bone analog was coated with fast-curing epoxy^g and high-temperature-resistant ceramic coating.^h The cancellous analog was positioned within the cortical bone silicone rubber mold by use of the built-in registration features (cubic extensions). Epoxy resin and hardener (100:23 ratio [wt/wt]) were used to prepare the cortical bone analog.ⁱ Variable amounts of glass fibers (measuring $20 \times 793 \mu\text{m}$) were mixed with the epoxy resin under 95% vacuum.^j Three groups of FRC replicas of radii were prepared with fiberglass-to-epoxy ratios (wt/wt) of 33%, 50%, or 60%. Each mixture was injected into the silicone rubber mold. The mold was placed inside a pressure chamber at 414 kPa (70 psi) for 1 hour while the resin set. After initial curing in the pressure chamber, the composite bone analogs were then cured at 75°C for 1 hour (Figure 2).

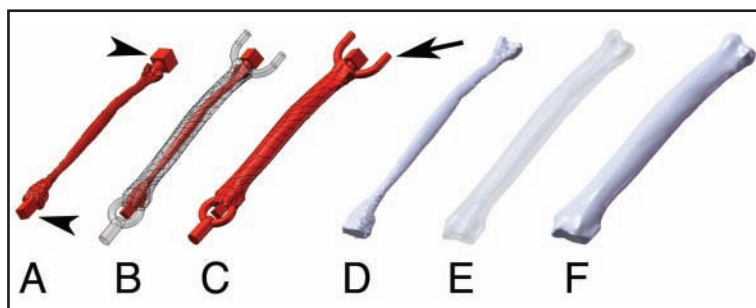


Figure 1—Three-dimensional illustrations of the cancellous core (A and D), transparent cortical shell (B and E), and outer surface (C and F) of an FRC replica of a canine radius. Molding sprues and locating features (cubic blocks [arrowheads]) have been added at the proximal and distal aspects of the cancellous core. The distal sprue allows injection of the polyurethane from the distal aspect of the bone. The cubic locating features ensure proper 3-D alignment of the cancellous core when it is placed in the mold used to inject the epoxy mixture. Tubular extensions are also present at the proximal aspect of the cortical shell (arrow). These tubes act as air vents, allowing the injection of the epoxy mixture without trapping air inside of the mold. The cancellous core and outer cortical shell are anatomically accurate after removal of the cubic and tubular extensions (D, E, and F).

Two identical molds were used to fabricate the 33% and 50% FRC replicas, and only one of these molds was used to fabricate the 60% FRC replicas.



Figure 2—Photograph of the cranial and lateral aspects of a 50% FRC replica of a canine radius. The epoxy-glass fiber mixture (in this instance, the fiberglass-to-epoxy ratio [wt/wt] was 50%) is transparent and free of visible bubbles. The replica length is 205 mm. Scale bars measure 20 mm.

Preliminary destructive mechanical testing—Sixteen cadaveric radii from 8 dogs were tested destructively in cranial bending, axial loading, or torsional bending by use of a materials testing machine.^k Yield and ultimate failure loads were recorded.

Nondestructive mechanical testing—Twenty-one FRC radii replicas and 5 cadaveric radii were tested nondestructively in random order in 4-point cranial bending, axial loading, and internal and external torsion by use of the materials testing machine.^k The loads for nondestructive testing were 40% of the yield loads measured during the preliminary destructive tests of cadaveric radii. The replicas and bones were loaded 4 times for all nondestructive bending, axial, and torsional tests. The first loading event in each mode was considered as a preconditioning load and was not used in the analyses. Load-displacement curves of the second, third, and fourth loading events were recorded, and the stiffnesses were calculated from the linear portion of the curves. Four-point bending tests were conducted on the cranial surfaces of the radii to loads of up to 500 N with a crosshead speed of 1.5 mm/min.¹⁹ For axial loading, the proximal and distal 2.12-cm portions of the replicas and radii were potted in epoxy cylinders measuring 2.54 cm (length) × 4.92 cm (diameter)^j and secured to the materials testing machine. The replicas and radii were loaded to 4,000 N with a crosshead speed of 1.5 mm/min. The torsional stiffness in internal and external rotation was measured by placing a torsional displacement of up to 10° on the replicas and radii at a rate of 6.5°/min.

Destructive mechanical testing—Fiberglass-reinforced composite replicas and cadaveric bones were tested to failure in 4-point bending. Yield loads, ultimate loads to failure, and modes of failure were recorded. Yield load was defined as a 1-mm offset from the linear portion of the curve. Failure was defined as a loss of stiffness or a deformation > 5 mm. The fractured surfaces of one of each type of FRC replica and a cadaveric bone were imaged with a digital 3-D microscope to subjectively assess the distribution of glass fibers.^l

Screw pullout—Mechanical testing was performed by use of the guidelines in the American Society for Testing and Materials standard for axial pullout load of medical bone screws.²⁰ Screw pullout was performed on

Table 1—Mean ± SD (coefficient of variation [%]) values of biomechanical variables of 3 replicas of a canine radius prepared with fiberglass-to-epoxy ratios (wt/wt) of 33%, 50%, or 60% (7 replicas/group) and cadaveric canine radii (5 bones).

Group	Axial stiffness (N/mm)	Bending stiffness (N/mm)	Internal torsional stiffness (N•mm/rad)	External torsional stiffness (N•mm/rad)	Ultimate bending load (N)	Ultimate screw pullout load (N)
Bone	1,758 ± 576 ^a (33)	377 ± 132 ^{a,b} (35)	50 ± 17 ^a (34)	48 ± 18 ^a (38)	1,482 ± 539 ^a (36)	1,650 ± 264 ^a (16)
33% FRC replica	2,250 ± 260 ^a (12)	320 ± 26 ^a (8)	73 ± 5 ^b (7)	75 ± 2 ^b (3)	1,350 ± 105 ^a (8)	1,966 ± 462 ^a (23)
50% FRC replica	3,383 ± 196 ^b (6)	456 ± 21 ^b (5)	94 ± 3 ^c (3)	99 ± 2 ^c (2)	1,353 ± 228 ^a (17)	2,212 ± 598 ^{a,b} (27)
60% FRC replica	4,067 ± 518 ^c (13)	668 ± 76 ^c (11)	130 ± 14 ^d (11)	134 ± 20 ^d (15)	1,243 ± 233 ^a (19)	2,875 ± 655 ^b (23)

By use of a materials testing machine, bones and FRC replicas underwent nondestructive mechanical testing including 4-point bending, axial loading, and torsion and destructive testing to failure during 4-point bending. Axial pullout loads for bone screws placed in the replicas and cadaveric radii were also assessed. Each mean value was derived from findings in 5 cadaveric bones or 7 replicas with the following exceptions: internal and external torsional stiffnesses for the 50% FRCs, n = 6; bending and internal torsional stiffnesses for the 60% FRCs, 6; and axial stiffness for the 60% FRCs, 5. Replicas were broken prior to or failed at some point during nondestructive testing.

^{a-c}Within a column, means with identical superscript letters do not differ significantly ($P \geq 0.05$).

a portion of the radial shaft that was not damaged in any of the replicas or radii during destructive mechanical testing. Seven 33% FRC replicas, seven 50% FRC replicas, four 60% FRC replicas, and 5 cadaveric radii were tested. Stainless steel 3.5-mm cortex screws^m were inserted in a craniocaudal direction in the proximal portion of the radial shaft. A jig was used for consistent screw placement by use of a 2.5-mm drill bit and a 3.5-mm tap. A tensile load was applied to the screw head at 1.5 mm/min until screw pullout or failure. The ultimate axial pullout load (maximum load of the load displacement curve) was recorded.

Statistical analysis—Stiffnesses were calculated from the load displacement curves. Axial, torsional, and flexural stiffnesses were compared by use of statistical software.ⁿ The second, third, and fourth loading events were compared within groups for all loading regimens by use of paired *t* tests after confirmation of normal distribution by use of the Shapiro-Wilk test for normality. The mean of the second, third, and fourth loading events was calculated and used for further analyses. The mean \pm SD and coefficient of variation were calculated for axial, torsional, and bending stiffnesses. Mean internal and external torsional stiffnesses were compared by use of a 1-way ANOVA. The mean bending stiffnesses, mean axial stiffnesses, and mean torsional stiffnesses of FRC replicas made from the 2 molds were compared by use of a 1-way ANOVA. The mean 4-point bending yields and ultimate loads to failure for all groups were analyzed by use of a 1-way ANOVA. Differences between groups were compared by use of Tukey-Kramer honestly significant difference tests. The mean ultimate loads leading to screw pullout were analyzed by use of a 1-way ANOVA. Differences between groups were compared by use of Tukey-Kramer honestly significant difference tests. Pearson correlation coefficients among testing regimens and between testing regimens and dog weight were calculated for cadaveric radii. Values of $P < 0.05$ were considered significant.

Results

The power analysis yielded sample sizes of 7 for all groups of FRC replicas. Twenty-six cadaver forelimbs were collected from 13 dogs; 16 limbs from 8 dogs were used for preliminary destructive tests, and 5 limbs randomly selected from 5 dogs were used for the non-destructive and destructive tests included in the main portion of this study. The postmortem mean \pm SD body weight of the 5 dogs used in the main part of the study was 38.5 ± 6.7 kg (range, 30 to 47 kg). No bones were excluded because of orthopedic abnormalities. For all mechanical tests, the mean, SD, and coefficient of variation for each group of replicas and the 5 cadaveric radii were calculated (Table 1).

Nondestructive axial compression—No conditioning effect over loading cycles was detected during axial compression. A 50% FRC replica broke before axial testing because of an operator error, and a 60% FRC replica failed during axial loading with a mid-diaphyseal transverse fracture. The mean axial stiffness was higher for 60% FRC replicas than that for 50% FRC

replicas ($P = 0.037$), 33% FRC replicas ($P < 0.001$), or cadaveric radii ($P < 0.001$). The 50% FRC replicas were stiffer than the 33% FRC replicas ($P < 0.001$) and cadaveric radii ($P < 0.001$). The mean axial stiffness of 33% FRC replicas and cadaveric radii did not differ ($P = 0.053$; power = 0.398).

Nondestructive torsional loading—With all groups combined, a conditioning effect from the second to fourth loading event (stiffness increase, 3.3%; $P = 0.043$) was identified in internal torsion. When individual groups were compared, internal torsion showed no conditioning effect (no significant differences between mean internal torsional stiffness of the fourth and second loading events) for the 33% FRC replicas (stiffness decrease, 1.6%; $P = 0.067$; power = 0.138), 50% FRC replicas (stiffness increase, 1.9%; $P = 0.074$; power = 0.164), 60% FRC replicas (stiffness increase, 5.2%; $P = 0.783$; power = 0.084), and cadaveric radii (stiffness increase, 9.9%; $P = 0.062$; power = 0.318). No conditioning effect over loading cycles was detected during external torsion. Two 60% FRC replicas failed in external torsion; one had a proximal metaphyseal spiral fracture, and the other had transverse fractures of the mid-diaphysis and proximal metaphysis. The mean internal torsional stiffness of the 60% FRC replicas was higher than that of the 50% FRC replicas ($P < 0.001$), 33% FRC replicas ($P < 0.001$), and cadaveric radii ($P < 0.001$). The 50% FRC replicas were stiffer than the 33% FRC replicas ($P = 0.004$) and cadaveric radii ($P < 0.001$). The internal torsional stiffness of the 33% FRC replicas did not differ significantly ($P = 0.176$; power = 0.549) from that of the cadaveric radii. The mean external torsional stiffness of the 60% FRC replicas was higher than that of the 50% FRC replicas ($P < 0.001$), 33% FRC replicas ($P < 0.001$), and cadaveric radii ($P < 0.001$). The 50% FRC replicas were stiffer than the 33% FRC replicas ($P = 0.006$) and cadaveric radii ($P < 0.001$). The 33% FRC replicas were stiffer than the cadaveric radii ($P = 0.004$). Internal and external tor-

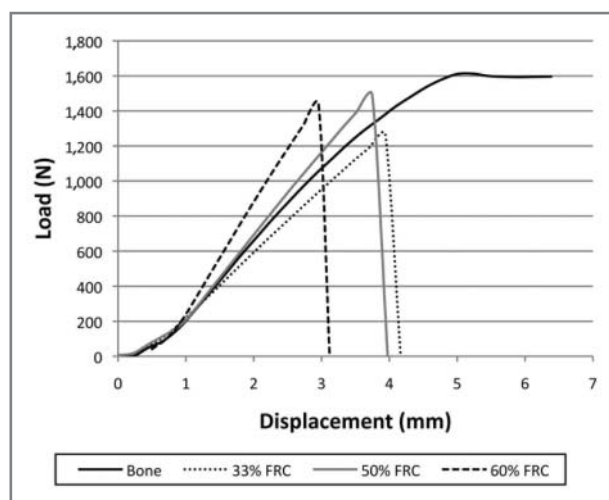


Figure 3—Representative load deformation 4-point bending curves for a cadaveric canine radius (bone) and 3 FRC replicas with 33%, 50%, and 60% glass fiber content. The bone and replicas were loaded to failure. The FRC replicas were more brittle than the bone and developed no signs of plastic deformation before failure.

Table 2—Pairwise correlations (r [P value]) between biomechanical variables determined by use of a materials testing machine and body weight of donor dogs for 5 cadaveric radii.

Variable	Weight	Bending stiffness	Axial stiffness	External torsional stiffness	Internal torsional stiffness
Weight	—	0.223 (0.718)	-0.335 (0.581)	0.118 (0.850)	0.103 (0.869)
Bending stiffness	—	—	0.684 (< 0.001)	0.743 (< 0.001)	0.740 (< 0.001)
Axial stiffness	—	—	—	0.843 (< 0.001)	0.833 (< 0.001)
External torsional stiffness	—	—	—	—	0.964 (< 0.001)

— = Not applicable.

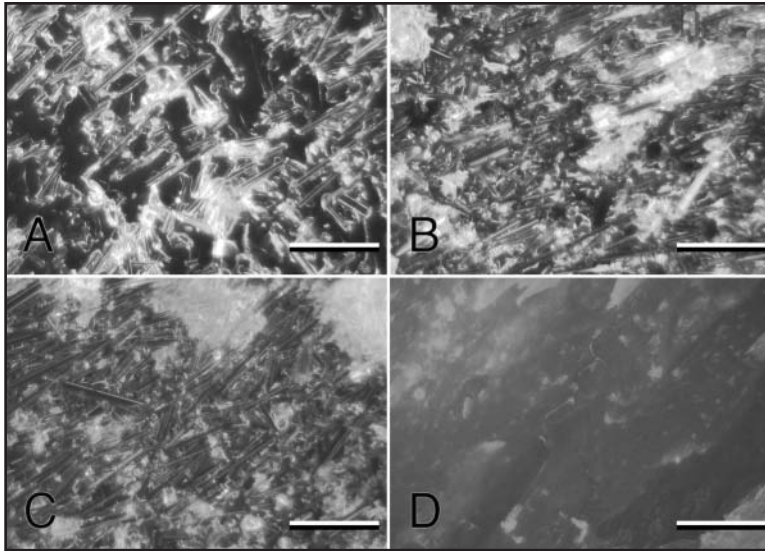


Figure 4—Three-dimensional photomicrographs of the unstained fractured surfaces of 33% (A), 50% (B), and 60% (C) FRC replicas and a cadaveric radius (D). The glass fibers are clearly visible and appear to be more concentrated for the 50% and 60% replicas than for the 33% replica. The fractured surface of the bone faintly shows obliquely oriented bone lamellae. In each panel, bar = 200 μ m.

sional stiffnesses did not differ significantly ($P = 0.142$; power = 0.231) from each other.

Nondestructive 4-point bending—No conditioning effect over loading cycles was detected during 4-point bending. Significant differences between group means were detected. The mean 4-point bending stiffness of 60% FRC replicas was higher than that of 50% FRC replicas ($P < 0.001$), 33% FRC replicas ($P < 0.001$), and cadaveric radii ($P < 0.001$; Figure 3). The 50% FRC replicas were stiffer ($P = 0.002$) than the 33% FRC replicas. The mean bending stiffness of the cadaveric radii did not differ significantly from that of the 33% FRC replicas ($P = 0.185$; power = 0.153) or 50% FRC replicas ($P = 0.073$; power = 0.253).

Intersample variability (coefficients of variation) among cadaveric radii was 2 to 19 times the findings among FRC replicas. Significant correlations were identified between the mechanical properties of cadaveric radii for all testing regimens, but were absent between these mechanical properties and the body weight of cadavers (Table 2). Fiberglass-reinforced composite replicas made with different molds did not differ significantly in mean axial stiffness ($P = 0.851$), mean bending stiffness ($P = 0.691$), mean internal torsional stiffness ($P = 0.944$), mean external torsional stiffness ($P = 0.692$), or ultimate loads to failure ($P = 0.588$).

Destructive 4-point bending—Mean yield load and ultimate load of cadaveric radii in 4-point bending were 959 ± 347 N and $1,482 \pm 539$ N, respectively. The FRC replicas had no detectable plastic deformation in 4-point bending and had identical yield loads and ultimate loads. The mean yield load in 4-point bending was higher for 50% and 33% FRC replicas than for cadaveric radii ($P = 0.042$ and 0.044 , respectively). The mean ultimate load in 4-point bending did not differ significantly between cadaveric radii and each group of FRC replicas ($P > 0.248$ for all comparisons) or among FRC replicas ($P > 0.563$). Replicas failed through transverse or short oblique mid-diaphyseal fractures. By comparison, the cadaveric bones underwent plastic deformation but did not fracture. Mean tensile load leading to screw pullout of the 60% FRC replicas was higher than that of the 33% FRC replicas ($P = 0.048$) and cadaveric radii ($P = 0.010$). The mean tensile load leading to screw pullout did not differ between 60% and 50% FRC replicas ($P = 0.200$; power = 0.326), between 50% and 33% FRC replicas ($P = 0.806$; power = 0.125), between 50% FRC replicas and cadaveric radii ($P = 0.271$; power = 0.468), and between 33% FRC replicas and cadaveric radii ($P = 0.719$; power = 0.256). Glass fibers were visible on the 3-D images of the fractured surfaces. They appeared more concentrated on the fractured surfaces of the 60% and 50% FRC replicas than on those of the 33% FRC replicas (Figure 4).

Discussion

The present study compared the mechanical properties of several replicas of a canine radius with each other and a group of cadaveric canine radii. The cancellous bone was replicated by use of polyurethane. Polyurethane cores have been used to replicate human cancellous bone.^{9,21} The cortical bone was replicated by use of epoxy with glass fibers. Epoxy-fiberglass mixtures have been used to replicate human cortical bone.^{8,12,13} The mechanical properties of the replicas were equal or superior to the mechanical properties of cadaveric radii. Also, the variability of the composite bone was equivalent (for screw pullout) or lower (for all other testing regimens) than the variability of cadaveric radii.

We accepted the hypothesis that composite radii could match the mechanical properties of canine radii while decreasing the variability of their mechanical

properties. When different groups of orthopedic constructs are compared, a lower variability among replicas, compared with the variability among cadaveric bones, has the advantage of enhancing the ability to detect differences between experimental groups of constructs. In other words, a smaller sample size would be required to detect differences between groups of orthopedic constructs if replicas were used instead of cadaveric bones. For example, if a group of bones had a 50% coefficient of variation, 242 bones would be required to detect a 20% difference between 2 groups of constructs with a power of 0.8. However, if a group of FRC replicas had a 5% coefficient of variation, only 12 FRC replicas would be necessary to detect the same difference with the same power. The use of replicas rather than cadaveric bone in biomechanical testing also offers the advantage of simultaneous comparisons of more than 2 experimental groups of constructs because paired comparisons are no longer necessary.²² Furthermore, cadaveric bones have several disadvantages. They are prone to dehydration. Hydrated bone maintains weak interfaces perpendicular to the collagen fibril axis, which helps inhibit crack propagation and aids in mechanical damping. Dehydrated bones lack these weak interfaces, resulting in an increase in modulus of elasticity and strength.²³ Wrapping bones with saline solution-soaked gauze sponges and placing them in sealed containers before freezing greatly decreases dehydration. In 1 study,²⁴ freezing for 1 year did not change the mechanical properties of goat femora and humeri. Specific cadaveric bones may be difficult to collect because of a lack of availability of some types of dogs. Cadaveric bones have highly variable mechanical properties. We did not identify a correlation between the mechanical properties of the cadaveric radii used in the study and the body weight of the donors. This suggests that the variability in mechanical properties of radii used in the study was not caused by differences in donor weights. The collection of bones from cadavers also raises ethical issues. Some organizations do not allow the collection of body parts from cadavers. The use of replicas for mechanical testing eliminates the ethical and logistic concerns associated with localization, collection, and storage of cadaveric bones.

The mechanical properties of the composite radii were clearly enhanced with increased glass fiber content. Therefore, we accepted the hypothesis that increasing glass fiber content would increase the axial, bending, and torsional stiffness of the replicas. Glass fibers and epoxy were easily mixed and injected during fabrication of the 33% and 50% FRC replicas. The fact that no 33% or 50% FRC replica failed during nondestructive testing and that there were narrow SDs for mean values in the 2 groups suggest that their fabrication process was uniform. The slurry resulting from mixing epoxy and glass fibers for the fabrication of the 60% FRC replicas, however, was subjectively much more viscous and made degassing, mixing, and injection into molds much more challenging. Although not confirmed, this challenging fabrication process could have been associated with a potential loss of uniformity in distribution of the glass fibers within the epoxy. Such potential nonuniformity was proposed as the likely

cause of the premature mechanical failures of three 60% FRC replicas during nondestructive testing. The use of industrial mixing and injection molding equipment would facilitate the fabrication of 60% FRC replicas. Although the increased stiffness of these replicas may make them less clinically relevant for the fabrication of canine radii or other similarly sized bones, that property could be useful in the fabrication of other replicas, including smaller or thinner bones. Also, replicas with tailored (ie, patient-specific) mechanical properties could be developed by varying the glass fiber content. Patient-specific replicas could be used to assess the stability and modes of failure of specific surgical procedures (eg, in the design of low-modulus implants in which mechanical properties should match the host bone).²⁵ The mechanical properties (Young modulus and ultimate strength) of a host bone can be estimated from quantitative CT scans.²⁶

In the present study, the mechanical properties of the 33% FRC replicas most closely approximated the mean stiffnesses of the cadaveric bones. However, the replicas had a higher external torsional stiffness. A higher torsional stiffness of replicas, compared with that of bones, was also identified in a study¹² involving human femora and tibiae. The lower torsional stiffness of bone, compared with that of the replicas, may result from the fact that the fibrolamellar bone of cadavers has a high degree of mechanical anisotropy.²² The composite material of replicas used in the present study most likely had lower anisotropy because the glass fibers appeared to be oriented mostly at random. A weakness in torsion, compared with bending, has also been reported for human long bones.²⁷ Even though this was not tested in the present study, we anticipate that replicas with a glass fiber content slightly < 33% would have a slightly lower torsional stiffness that would match the torsional stiffness of bone. Internal and external torsional stiffnesses of cadaveric radii and replicas were very similar. Loads resulting in screw pullout were higher in the 60% FRC replicas than those in bones. Similar to our findings, the pullout load of 3.5-mm-diameter cortical screws placed in FRC replicas was equal to or larger than (depending on the diameter of the medullary cavity of the replicas) the pullout load of cadaveric bones in a study²⁸ of human femora. Even though increased glass fiber content increased bending stiffness, it did not increase ultimate bending load. This may be because the ultimate bending load was linked to the failure characteristics of the cured epoxy resin matrix. The presence of short-length glass fiber in composites has been shown to reduce crack propagation within the epoxy resin matrix,¹³ but the impact of changes in short-length glass fiber content on crack propagation for the bone tested in the present study is not known. The replicas were more brittle than the cadaveric bones; they failed abruptly, without noticeable plastic deformation.

In developing the FRC replica manufacturing process, we noted the presence of small bubbles within the epoxy during the early fabrication steps. Bubbles may have resulted from aeration during mixing, gas production during the exothermic polymerization of the epoxy, or the reaction between epoxy and the polyurethane core. Bubbles create a disruption in the uniformity of the epoxy resin and serve as a nidus for crack initiation and propaga-

tion and premature mechanical failure. Several steps were implemented that successfully avoided the presence of bubbles: we coated the polyurethane foam core with a thin layer of epoxy to seal pores in the foam and with a layer of heat-resistant ceramic paint, mixed the epoxy and fibers under vacuum to degas the mixture, and cured the epoxy in a pressure chamber.

Results of the present study indicated that epoxy composite radii reinforced with short-length glass fibers are an alternative to the use of cadaveric radii for biomechanical studies. The 33% FRC replicas appeared to be the best alternative to cadaveric bones when testing constructs involving the radii of large dogs. The intersample variability of FRC replicas was lower than the variability among cadaveric bones. Changes in the amount of glass fibers in replicas altered the mechanical properties of the bones, potentially allowing researchers to use FRC replicas to study orthopedic procedures intended for patients with specific bone problems, including osteoporosis. Future research could include the assessment of the impact of glass fiber length on the mechanical properties of FRC replicas and the development and validation of replicas for other bones.

- a. G*power 3.1, Christian-Albrechts-Universität, Kiel, Germany.
- b. Siemens SOMATOM Sensation 16-slice configuration, Siemens Medical Solutions, Malvern, Pa.
- c. Mimics, version 8.11, Materialize, Ann Arbor, Mich.
- d. Alaris polyjet 3-D printer, Objet Geometries Ltd, Billerica, Mich.
- e. Shore 60A, Smooth-on, Easton, Pa.
- f. 16 LB Density Urethane Foam, U.S. Composites Inc, West Palm Beach, Fla.
- g. Loctite Professional Epoxy 5 MIN, Henkel Corp, Rocky Hill, Conn.
- h. VHT Flameproof Coating, DupliColor Inc, Cleveland, Ohio.
- i. System 2000 Epoxy Resin and 2020 Epoxy Hardener, Fibre Glast Developments Corp, Brookville, Ohio.
- j. Milled glass fiber, U.S. Composites Inc, West Palm Beach, Fla.
- k. ATS 1620C, Applied Test Systems, Butler, Pa.
- l. KH-7700, Hirox-USA Inc, River Edge, NJ.
- m. Synthes Inc, West Chester, Pa.
- n. JMP, version 8.0, SAS Institute Inc, Cary, NC.

References

1. Benson CV, An YH. Basic facilities and instruments for mechanical testing of bone. In: An YH, Draughn RA, eds. *Mechanical testing of bone and bone-implant interface*. Boca Raton, Fla: CRC Press, 1999;87–102.
2. Dunlap JT, Chong AC, Lucas GL, et al. Structural properties of a novel design of composite analogue humeri models. *Ann Biomed Eng* 2008;36:1922–1926.
3. Markel MD, Sielman E, Rapoff AJ, et al. Mechanical properties of long bones in dogs. *Am J Vet Res* 1994;55:1178–1183.
4. Ricalde P, Caccamese J, Norby C, et al. Strength analysis of 6 resorbable implant systems: does heating affect the stress-strain curve? *J Oral Maxillofac Surg* 2008;66:2493–2497.
5. Hammel SP, Elizabeth Pluhar G, Novo RE, et al. Fatigue analysis of plates used for fracture stabilization in small dogs and cats. *Vet Surg* 2006;35:573–578.
6. Murphy TP, Hill CM, Kapatkin AS, et al. Pullout properties of 3.5-mm AO/ASIF self-tapping and cortex screws in a uniform synthetic material and in canine bone. *Vet Surg* 2001;30:253–260.
7. Marcellin-Little DJ, Roe SC, Rovesti GL, et al. Are circular external fixators weakened by the use of hemispheric washers? *Vet Surg* 2002;31:367–374.
8. Heiner AD. Structural properties of fourth-generation composite femurs and tibias. *J Biomech* 2008;41:3282–3284.
9. Szivek JA, Thomas M, Benjamin JB. Characterization of a synthetic foam as a model for human cancellous bone. *J Appl Biomater* 1993;4:269–272.
10. Cristofolini L, Viceconti M, Cappello A, et al. Mechanical validation of whole bone composite femur models. *J Biomech* 1996;29:525–535.
11. Cristofolini L, Viceconti M. Mechanical validation of whole bone composite tibia models. *J Biomech* 2000;33:279–288.
12. Heiner AD, Brown TD. Structural properties of a new design of composite replicate femurs and tibias. *J Biomech* 2001;34:773–781.
13. Chong AC, Miller F, Buxton M, et al. Fracture toughness and fatigue crack propagation rate of short fiber reinforced epoxy composites for analogue cortical bone. *J Biomech Eng* 2007;129:487–493.
14. Lorinson K, Loebcke S, Skalicky M, et al. Signalment differences in bone mineral content and bone mineral density in canine appendicular bones. A cadaveric study. *Vet Comp Orthop Traumatol* 2008;21:147–151.
15. Faul F, Erdfelder E, Lang AG, et al. G*Power 3: a flexible statistical power analysis program for the social, behavioral, and biomedical sciences. *Behav Res Methods* 2007;39:175–191.
16. Marcellin-Little DJ, Harrysson OL, Cansizoglu O. In vitro evaluation of a custom cutting jig and custom plate for canine tibial plateau leveling. *Am J Vet Res* 2008;69:961–966.
17. Bredenhöller C, Feuerlein U. *SOMATOM Sensation 10/16 application guide*. 2nd ed. Munich: Siemens AG, 2005;580.
18. Bredenhöller C, Feuerlein U. *SOMATOM Sensation 10/16 application guide*. 2nd ed. Munich: Siemens AG, 2005;73.
19. Jain R, Podworny N, Hearn T, et al. A biomechanical evaluation of different plates for fixation of canine radial osteotomies. *J Trauma* 1998;44:193–197.
20. American Society for Testing and Materials. ASTM designation F 543-07. Standard specification and test methods for metallic medical bone screws. In: *Annual book of ASTM standards*. 7th ed. West Conshohocken, Pa: American Society for Testing and Materials, 2007;1–20.
21. Patel PS, Shepherd DE, Hukins DW. Compressive properties of commercially available polyurethane foams as mechanical models for osteoporotic human cancellous bone. *BMC Musculoskelet Disord* 2008;9:137.
22. Hildreth BE, Marcellin-Little DJ, Roe SC, et al. In vitro evaluation of five canine tibial plateau leveling methods. *Am J Vet Res* 2006;67:693–700.
23. Seto J, Gupta HS, Zaslansky P, et al. Tough lessons from bone: extreme mechanical anisotropy at the mesoscale. *Adv Function Mat* 2008;18:1905–1911.
24. van Haaren EH, van der Zwaard BC, van der Veen AJ, et al. Effect of long-term preservation on the mechanical properties of cortical bone in goats. *Acta Orthop* 2008;79:708–716.
25. Harrysson OLA, Cansizoglu O, Marcellin-Little DJ, et al. Direct metal fabrication of titanium implants with tailored materials and mechanical properties using electron beam melting technology. *Mater Sci Eng C* 2008;28:366–373.
26. Duchemin L, Bousson V, Raoussanly C, et al. Prediction of mechanical properties of cortical bone by quantitative computed tomography. *Med Eng Phys* 2008;30:321–328.
27. Miyasaka Y, Sakurai M, Yokobori AT Jr, et al. Bending and torsion fractures in long bones (a mechanical and radiologic assessment of clinical cases). *Biomed Mater Eng* 1991;1:3–10.
28. Zdero R, Elfallah K, Olsen M, et al. Cortical screw purchase in synthetic and human femurs. *J Biomech Eng* 2009;131:094503.